

## Evolution of Single-Particle Energies for N=9 Nuclei at Large N/Z

A. H. Wuosmaa<sup>1</sup>, S. Bedoor<sup>1</sup>, M. Alcorta<sup>2</sup>, B. B. Back<sup>2</sup>, B. A. Brown<sup>3</sup>, C. M. Deibel<sup>4</sup>, C. R. Hoffman<sup>2</sup>, J. C. Lighthall<sup>1,2</sup>, S. T. Marley<sup>1,2</sup>, R. C. Pardo<sup>2</sup>, K. E. Rehm<sup>2</sup>, A. M. Rogers<sup>2</sup>, J. P. Schiffer<sup>2</sup>, D. V. Shetty<sup>1</sup>

<sup>1</sup>Department of Physics, Western Michigan University, Kalamazoo, MI 49024-5252 USA

<sup>2</sup>Physics Division, Argonne National Laboratory, Argonne, IL 60439 USA

<sup>3</sup>Department of Physics and Astronomy, Michigan State University, E. Lansing, MI 48824 USA

<sup>4</sup>Department of Physics and Astronomy, Louisiana State University, Baton Rouge LA 70803, USA

**Abstract.** We have studied the nucleus  $^{14}\text{B}$  using the  $^{13}\text{B}(d,p)^{14}\text{B}$  and  $^{15}\text{C}(d,^3\text{He})^{14}\text{B}$  reactions. The two reactions provide complementary information about the negative-parity  $1s_{1/2}$  and  $0d_{5/2}$  neutron single-particle states in  $^{14}\text{B}$ . The data from the  $(d,p)$  reaction give neutron-spectroscopic strengths for these levels, and the  $(d,^3\text{He})$  results confirm the existence of a broad  $2^-$  excited state suggested in the literature. Together these results provide estimates of the  $sd$ -shell neutron effective single-particle energies in  $^{14}\text{B}$ .

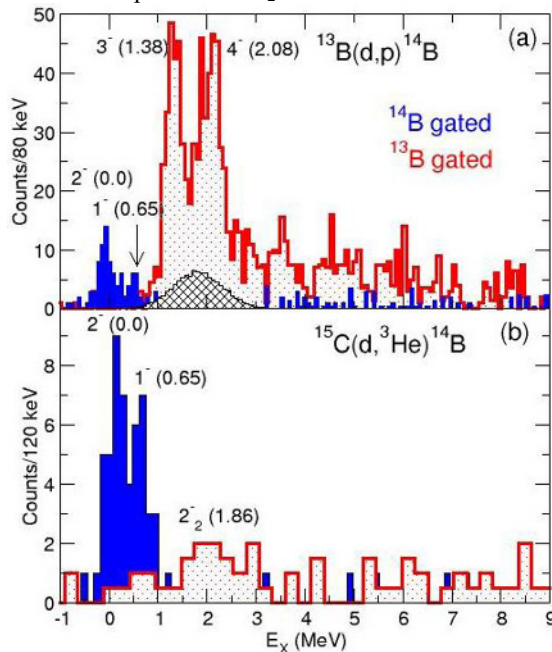
The effective single-particle energies (ESPE) of shell-model orbitals are crucial ingredients for nuclear-structure calculations. In shell-model calculations they set the scale for excitation energies, as well as help determine the degree of configuration mixing for multi-particle states. The ESPE depend on the filling of neutron and proton orbitals, and it is particularly interesting to determine how the values of these energies evolve as a function of N/Z, especially at the limits of nuclear stability.

In light nuclei, the values of the ESPE are sensitive to many aspects of the nuclear force responsible for modifications in heavier systems, such as the tensor force [1,2]. The nucleus  $^{14}\text{B}$ , with a neutron separation energy of 0.969 MeV, is the lightest bound N=9 isotone. With a single neutron outside the closed  $p$  shell it provides an excellent opportunity to track the  $1s_{1/2}$  and  $0d_{5/2}$  ESPE to, and beyond, the limits of stability. There exists a well-known inversion between these two orbitals moving from  $^{17}\text{O}$  to  $^{15}\text{C}$ , and we wish to learn how the energies of these orbitals evolve in  $^{14}\text{B}$ . To study this evolution, we have investigated the structure of  $^{14}\text{B}$  using two nucleon-transfer reactions: neutron adding with  $^{13}\text{B}(d,p)^{14}\text{B}$ , and proton removal with  $^{15}\text{C}(d,^3\text{He})^{14}\text{B}$ . These two reactions provide complementary information about  $^{14}\text{B}$  and together, the results provide information that can be used to determine the  $sd$ -shell ESPE in  $^{14}\text{B}$ .

Our measurements were conducted using the HELical Orbit Spectrometer (HELIOS) [3,4] at the ATLAS facility at Argonne National Laboratory. HELIOS is a device specifically designed to study reactions in inverse kinematics. HELIOS utilizes the uniform magnetic field produced by a large solenoid magnet to transport light-charged particles from the target to an array of position-sensitive silicon detectors. The magnetic-field axis is aligned with the beam direction, and the target and silicon-detector array also lie on this axis. Conceptual and operational details about HELIOS may be found in [3,4]. In our measurements, unstable  $^{13}\text{B}$  and  $^{15}\text{C}$  beams were produced from a primary  $^{14}\text{C}$  beam at 17.1 MeV/u, using the  $^{14}\text{C}(^9\text{Be},^{10}\text{B})^{13}\text{B}$  and  $^{14}\text{C}(d,p)^{15}\text{C}$  reactions, respectively, using the in-

flight production facility at Argonne National Laboratory [5]. The light-charged particles ( $^3\text{He}$  and  $p$ ) were detected in the HELIOS silicon-detector array. For the  $(d,p)$  reaction, the interesting protons are emitted at backward ( $\theta_{\text{lab}} > 90^\circ$ ) angles, whereas  $^3\text{He}$  particles from the  $(d,^3\text{He})$  reaction go to forward angles in the laboratory. The forward-going  $^{13,14}\text{B}$  particles from unbound, and bound states in  $^{14}\text{B}$  were detected and identified in silicon-detector telescopes at the downstream end of HELIOS. The  $^{14}\text{B}$  excitation energy is deduced from the correlation between the energy and the position of the detected light charged particle as described in [3,4].

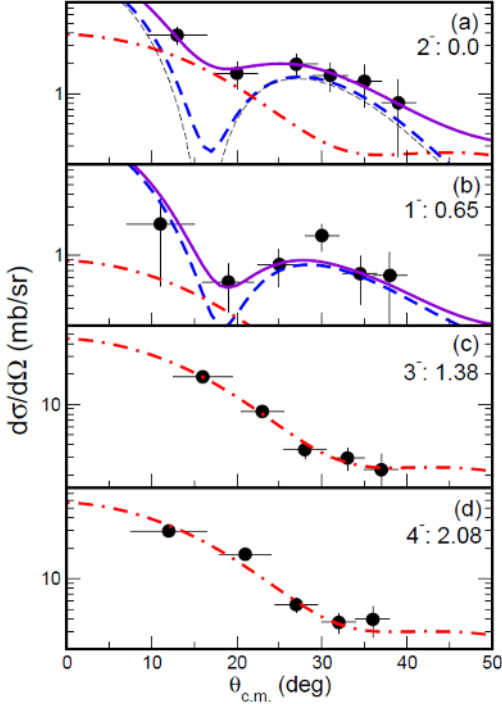
Figure 1 shows  $^{14}\text{B}$  excitation-energy spectra for the  $^{13}\text{B}(d,p)^{14}\text{B}$  (a) and  $^{15}\text{C}(d,^3\text{He})^{14}\text{B}$  (b) reactions. The filled (open) histograms represent events where the proton or  $^3\text{He}$  was detected in coincidence with identified  $^{14}\text{B}$  ( $^{13}\text{B}$ ) ions, corresponding to bound(unbound) states in  $^{14}\text{B}$ . In  $^{14}\text{B}$ , low-lying negative-parity states are formed by coupling  $1s_{1/2}$  or  $0d_{5/2}$  neutrons to a  $0p_{3/2}$  proton hole, and compilations [6] give a sequence of  $(2,1,3,2,4)^-$  states, determined largely from a study of the  $^{14}\text{C}(^7\text{Li},^7\text{Be})^{14}\text{B}$  reaction and a comparison to known levels in  $^{12}\text{B}$  [7]. The  $(2,1,1,3,1,4)^-$  states are observed in the  $(d,p)$  reaction, although the measurement is probably insensitive to the broad excited  $2_2^-$  state as it would be buried beneath the much stronger  $3_1^-$  and  $4_1^-$  excitations. The cross-hatched histogram in Fig. 1(a) shows an estimate of how the  $2_2^-$  level would appear in our data. A broad  $1_2^-$  state is expected at higher excitation energy; however such a level is not conclusively identified in the spectrum. Due to the  $1s_{1/2}$  neutron single-particle nature of  $^{15}\text{C}$ , only states in  $^{14}\text{B}$  with  $1s_{1/2}$  spectroscopic strength should be populated in the  $(d,^3\text{He})$  reaction. The  $^{14}\text{B}$  excitation-energy spectrum from that reaction in Fig. 1(b) contains only the ground and first-excited states, and a weak, broad bump that appears near 2 MeV. Although the statistics are small, the data are reasonably clean and we tentatively associate this bump with the  $2_2^-$  state at 1.86 MeV in the literature.



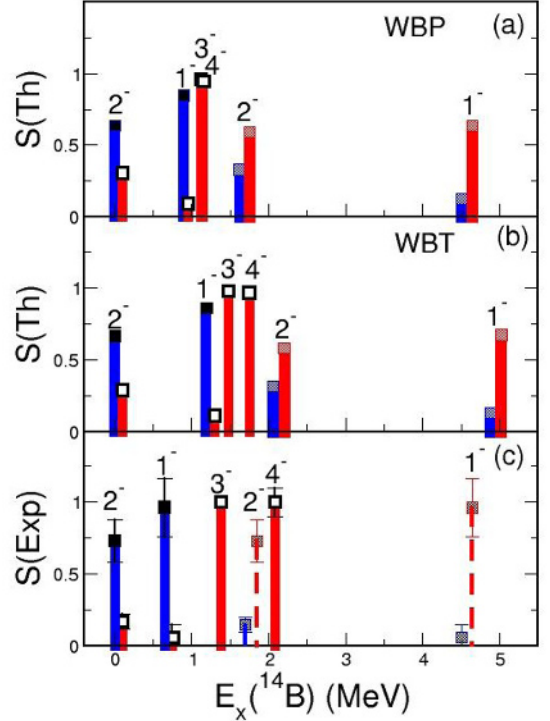
**Figure 1.** Excitation-energy spectra for the  $^{13}\text{B}(d,p)^{14}\text{B}$  (a) and  $^{15}\text{C}(d,^3\text{He})^{14}\text{B}$  (b) reactions.

Figure 2 shows angular distributions for the four narrow states observed in the  $^{13}\text{B}(d,p)^{14}\text{B}$  reaction, plotted with curves from distorted-wave Born-Approximation calculations. The optical-model parameters reproduce proton and deuteron elastic scattering from  $^{12,13}\text{C}$  at the same bombarding energy and are given in Ref. [8]. For the  $2_2^-$  and  $1_1^-$  states, both  $l=0$  and  $2$  are permitted, and the dashed and dot-dashed curves represent  $l=0$ , and  $2$ , respectively. The solid curves shows the sum of  $l=0+2$  determined from a best fit to the data. The  $3_1^-$  and  $4_1^-$  angular distributions are well described by pure  $l=2$  transitions as expected.

Spectroscopic factors (SF) deduced from comparisons between the data and the DWBA calculations are plotted in Fig. 3, which also shows the values from shell-model calculations using the WBP and WBT interactions [9]. Here, the SF deduced from the experiment are normalized such that the value of  $S(3^-)=1.0$ . Uncertainties are determined from the least-squares fitting procedure. The agreement between the calculated and deduced relative SF for the observed states is excellent.



**Figure 2.** Angular distributions for the  $^{13}\text{B}(d,p)^{14}\text{B}$  reaction. The curves are described in the text.



**Figure 3.** Experimental and theoretical SF for  $^{14}\text{B}$ . Filled(open) symbols correspond to  $l=0(2)$ .

Although the  $2^-$  and  $1^-$  excitations are not observed in the  $^{13}\text{B}(d,p)^{14}\text{B}$  reaction, it is possible to estimate their SF under the assumptions that the  $(2^-_1, 2^-_2)$  and  $(1^-_1, 1^-_2)$  levels are pairs of orthogonal states mixed by the residual interaction, and that  $0d_{3/2}$  neutrons are irrelevant at low excitation energies. In that case, the SF for the unobserved levels can be determined from those of the observed states. These values are indicated by the dashed lines in Figure 3(c). The weak population of the  $2^-$  state in the  $(d,^3\text{He})$  reaction seen in Figure 1(b) is consistent with the small  $1s_{1/2}$  SF inferred from the  $(d,p)$  data. From the  $(d,p)$  reaction, we find that the  $1^-_1$  first-excited state is essentially pure  $l=0$ , and thus the  $1^-_2$  state would have little or no strength in the  $(d,^3\text{He})$  reaction.

With the SF determined for the low-lying  $1s_{1/2}$  and  $0d_{5/2}$  neutron states determined from the  $(d,p)$  reaction, and the  $2^-$  state confirmed from the  $(d,^3\text{He})$  reaction, we can estimate the ESPE of those orbitals from the centroid of the SF-weighted excitation energies, also weighted by the  $(2J+1)$  statistical factor (See Ref. [10]). Here, as the energy of the  $1^-_2$  excitation is still unknown, we assign it the value of  $E_x(1^-_2)=4.5$  MeV from the WBT calculation, although due to the small  $1s_{1/2}$  SF and low spin this precise value has little influence on the final ESPE values. The ESPE for  $N=9$  isotones from  $^{17}\text{O}$  to  $^{13}\text{Be}$  are plotted in Fig. 4, with the results for  $^{16}\text{N}$  and  $^{13}\text{Be}$  taken from the work of Bohne *et al.* [11], and Simon *et al.* [12], respectively. The present results for  $^{14}\text{B}$  fit the trends established by the other nuclei extremely well. The corresponding values from the WBP and WBT calculations, as well as from a new calculation from Yuan *et al.* [13] are shown as the solid, dashed, and dotted horizontal lines in Fig. 4. In addition to better reproducing the  $1s_{1/2}$ - $0d_{5/2}$  splitting, this recent interaction is in

better agreement than WBT or WBP with the observed level ordering of the low-lying states in  $^{14}\text{B}$  [13], with the  $2^-_2$  level appearing between the  $3^-_1$  and  $4^-_1$  in agreement with tentative assignments.

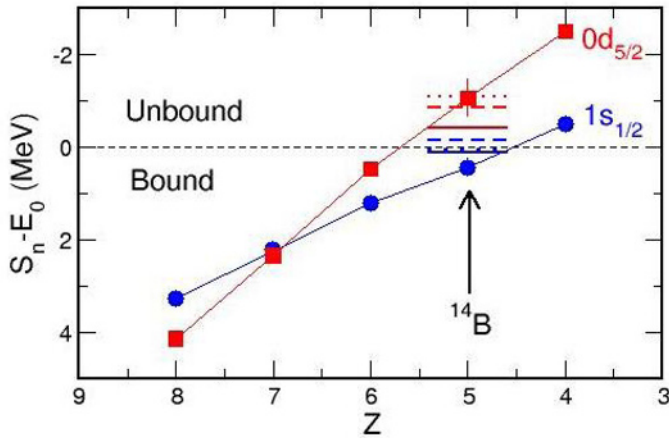


**Figure 4.** Effective single-particle energies for  $N=9$  isotones as a function of  $Z$ .

In summary, we have studied the  $^{13}\text{B}(d,p)^{14}\text{B}$  and  $^{15}\text{C}(d,^3\text{He})^{14}\text{B}$  reactions in inverse kinematics using HELIOS. The results indicate that the ground and first-excited states are largely dominated by  $1s_{1/2}$  neutron configuration. Relative SF for the four low-lying narrow negative-parity states are in good agreement with the predictions of shell-model calculations. Preliminary data for the  $(d,^3\text{He})$  reaction support the presence of a broad  $2^-$  excited state. With some assumptions about the structures of the low-lying levels we obtain estimates of the neutron ESPE in  $^{14}\text{B}$  which are well in line with the trend established by other nearby  $N=9$  nuclei. More details about the  $^{13}\text{B}(d,p)^{14}\text{B}$  measurement can be found in Ref. [14].

This work was supported by the U. S. Department of Energy under contract numbers DE-FG02-04ER41320 and DE-AC02-06CH11357, and the U. S. National Science Foundation under Grant number PHY-1068217.

## References

1. Takaharu Otsuka *et al.*, Phys. Rev. Lett. **87**, 082502 (2001)
2. T. Otsuka, T. Suzuki, R. Fujimoto, H. Grawe, and Y. Akaishi, Phys. Rev. Lett. **95**, 232502 (2005)
3. A. H. Wuosmaa *et al.*, Nucl. Instr. and Meth. in Phys. Res. A, **580**, 1290 (2007)
4. J. C. Lighthall *et al.*, Nucl. Instr. and Meth. in Phys. Res. A, **622**, 97 (2010)
5. B. Harss *et al.*, Rev. Sci. Instrum. **71**, 380 (2000)
6. F. Azjenberg-Selove, Nucl. Phys. A **523**, 1 (1991)
7. G. C. Ball *et al.*, Phys. Rev. C **33**, 395 (1973)
8. H. Ohnuma *et al.*, Nucl. Phys. A **448**, 205 (1986) and J. S. Petler *et al.*, Phys. Rev. C **32**, 673 (1985)
9. B. A. Brown and B. H. Wildenthal, Phys. Rev. C **46**, 923 (1992)
10. W. Bohne *et al.*, Nucl. Phys. A **196**, 41 (1972)
11. H. Simon *et al.*, Nucl. Phys. A **791**, 267 (2007)
12. M. Baranger, Nucl. Phys. A **149**, 225 (1970)
13. C. Yuan *et al.*, Phys. Rev. C **85**, 064324 (2012)
14. S. Bedoor *et al.*, Phys. Rev. C. **88**, 011304(R) (2013)